Stabilization of thermoacoustic system through multipartitioned burner design with its corresponding flame

30th International Congress on Sound and Vibration

ICSV30 AMSTERDAM 8-11 JULY 2024

STABILIZATION OF THERMOACOUSTIC SYSTEM THROUGH MULTI-PARTITIONED BURNER DESIGN WITH ITS CORRESPONDING FLAME

Hamed F. Ganji
Department of Mechanical Engineering, Eindhoven University of Technology, the Netherlands.
E-mail: h.faghanpourganji@tue.nl
Viktor Kornilov
Department of Mechanical Engineering, Eindhoven University of Technology, the Netherlands.
E-mail: v.kornilov@tue.nl
Jeroen van Oijen
Department of Mechanical Engineering, Eindhoven University of Technology, the Netherlands.
E-mail: j.a.v.oijen@tue.nl
Ines Lopez Arteaga
Department of Mechanical Engineering, Eindhoven University of Technology, the Netherlands.
Department of Engineering Mechanics, KTH Royal Institute of Technology, Sweden.
E-mail: i.lopez@tue.nl
Philip de Goey
Department of Mechanical Engineering, Eindhoven University of Technology, the Netherlands.
E-mail: l.p.h.d.goey@tue.nl

Abstract

Thermoacoustic instability within combustion systems is heavily influenced by the thermoacoustic characteristics of the burner in conjunction with its flame. A promising strategy to mitigate these instabilities involves targeting the thermoacoustic properties of the burner itself. One innovative approach for modifying or designing the burner with its corresponding flame is grounded in the heuristic notion that the acoustic response of one flame (with burner) can be counterbalanced by the appropriately tuned response of other flames. In the case of premixed gaseous multiple Bunsen-type flames anchored to the burner deck with perforations, this concept suggests the integration of various sizes and shapes of perforations in burners. However, without prior knowledge, this approach often necessitates extensive trial and error, leading to excessive costs in the Research and Development (R&D) process. Achieving a burner design and its corresponding flame that operate thermo-acoustically stable within the combustion system, while also meeting additional requirements such as emissions, operational durability, mechanical resilience, modulation rate, and others, poses a significant challenge. In this study, we initially articulate the concept of the burner transfer matrix (TM) composition to allows us to predict the TM of complex composite burners on basis of TM of its constituting parts. Then, we establish the complete framework of burner-flame TM composition based on a tabulated library of elemental burners' pressure drop (PD), elemental burners TM, and elemental flame Transfer Functions (TF). To illustrate this design methodology, we analyze a duct-flame-duct case study. Finally, we present a stability chart that delineates thermo-acoustically safe and unsafe combinations of segments/partitions, offering valuable insights into the R&D process of burner development. By leveraging such a stability chart and considering other operational constraints, designers can systematically achieve optimized designs.

Keywords: Thermoacoustic instability, Composite burner design, Transfer matrix composition

1. Introduction

Thermoacoustic instability poses risks of disruptive noise and potential physical damage to combustion appliances, prompting extensive research into its prediction and control strategies [1]. One interesting approach focuses on designing an acoustically stable combustor tailored to the given upstream/downstream acoustics. This can be achieved, for instance, by varying the sizes and shapes of perforations within the burner [2, 3]. The underlying concept behind this approach is based on the heuristic notion that the acoustic response of one flame type can be partly compensated or canceled out by other flame types.
In this study, our aim is to investigate the viability of employing different perforation combinations in a burner to design a burner with specific acoustic properties for mitigating thermoacoustic instability.

Significant progress has been made in understanding the formation of flame transfer functions (TF) and identifying key parameters influencing thermoacoustic response in burners [4]. However, there has been limited emphasis on the practical application of these concepts in the systematic design of burners. Kagiya [5] proposed an initial approach by suggesting the selection of a mixed perforation pattern, where the TF phase of one group of holes opposes the TF phase of a second group at the onset of instability. In a study by Kornilov et al. [2], a superposition approach was proposed to decompose the transfer function (TF) of multiple groups of laminar Bunsen flames. Two decomposition hypotheses were investigated to divide the composite pattern into two burner decks. The first hypothesis involved directly dividing the composite pattern into two equal-perforation burner decks with the same flame spacing (pitch). The second hypothesis involved dividing the composite pattern into two uniformly perforated burner decks with equal open area (burner porosity), denoted as equal p/D, where p and D represent the perforation pitch and diameter, respectively. Through a series of measurements, the second hypothesis was found to provide better predictions of global flame TF.
In a recent study, Ganji et al. [6] expanded upon this concept, exploring a broader range of thermal powers and investigating two distinct configurations for composite burners: mixed-perforation and partitioned burners. They found that, due to the mutual interaction of flames and the influence of flame foot motion at a global level, flame spacing (pitch) plays a critical role in shaping the composite transfer function. Consequently, the partitioned burner concept demonstrated superior predictability of the accumulated flame TF compared to the mixed-perforation burner across the entire thermal power spectrum. The partitioned composite burner configuration offers flexibility in determining the total area occupied by holes in each elemental burner, resulting in more predictable and efficient designs. This advantage underscores the superiority of the partitioned configuration over the mixed-perforation pattern. However, modifications in burner design may significantly affect the acoustic properties of the burner regardless of its corresponding flame, a concern that has not been thoroughly addressed in previous works. In our current study, we aim to bridge this gap by introducing the concept of burner Transfer Matrix (TM) composition. By manipulating the burner-flame composition and distribution through the burner perforation pattern, our objective is to develop a tailored burner-flame transfer matrix (TM) capable of mitigating thermoacoustic instability. This exploration introduces a pioneering framework for addressing thermoacoustic instabilities in combustion systems. To illustrate this multi-step procedure, we provide a numerical example based on a duct-flame-duct test case. Ultimately, this approach opens up the possibility of systematically achieving the most optimized design.
This article is organized as follows: Section 2 contains a brief overview of the main characteristics of the thermoacoustic system based on the network modeling approach. The rest of Section 2 is devoted to the elaboration of the framework of burner-flame composition in order to open the opportunity to design modified complex burners on basis of the characteristics of their different segments/partitions. Section 3 contains the main results of the paper. We use the duct-flame-duct test case, to demonstrate the validity and ability of the discussed framework to serve as a toolbox in prediction and design of flame-acoustic coupling in burners. After a brief recap of the main concepts, we formulate conclusions and perspectives.

2. Methodology & Experimental method

2.1 Formulation of dispersion relation in a generic combustion system

To employ one-dimensional linear acoustic network modeling, it is essential that the frequency range of interest remains smaller than the cut-off frequency of the first transverse mode [7], a condition typically applicable in thermoacoustics. Various options exist for the variables used to articulate the transfer matrices of the elements. Here let us focus on the Riemann invariants f_j and g_j where are written in terms of the complex acoustic pressure p'_j and the acoustic particle velocity u'_j. Where $j = 1, 2$, and the number 1 and 2 indicate upstream and downstream, respectively. At the limit of zero Mach number, we have

$$f_j = 0.5\Big(\frac{p'_j}{z_j} + u'_j\Big), \qquad g_j = 0.5\Big(\frac{p'_j}{z_j} - u'_j\Big), \tag{1}$$

where characteristic impedance can be defined as $z_j = \rho_{0j} c_{0j}$ and ρ_{0j} and c_{0j} are respectively the densities and speed of sound in the fluid [7]. Note that values of ρ_{0j} and c_{0j} are different at up/down -stream of the burner. When the forward and backward travelling waves at one (physical) side of the element are written as a function of the ones at the other side, interrelations which involves a so-called the transfer matrix $\mathbf{T}$ is obtained:

$$\begin{bmatrix} f_2 \\ g_2 \end{bmatrix} = \overbrace{\begin{bmatrix} T_{11} & T_{12} \\ T_{21} & T_{22} \end{bmatrix}}^{[\mathbf{T}]} \begin{bmatrix} f_1 \\ g_1 \end{bmatrix}, \tag{2}$$

For the abstract model in terms of the transfer matrix T, shown in Figure 1, the total set of system equations is given by [8],

$$\begin{bmatrix} -1 & R_{up} & 0 & 0 \\ T_{11} & T_{12} & -1 & 0 \\ T_{21} & T_{22} & 0 & -1 \\ 0 & 0 & R_{dn} & -1 \end{bmatrix} \begin{bmatrix} f_1 \\ g_1 \\ f_2 \\ g_2 \end{bmatrix} = 0. \tag{3}$$

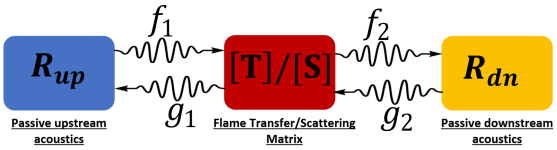

Figure 1: Generic 1D acoustic network model of a combustion system.

Note that all entries T_{ij}, upstream reflection coefficient R_{up} and downstream reflection coefficient R_{dn} may be functions of the Laplace variable ($s = i\omega + \sigma$) on the basis of time dependency in the form e^{st} in the governing equations. The ω indicates angular frequency and is defined as $2\pi f$, where f indicates the eigen-frequency. The σ indicates the oscillations grow/decay rate [8]. This homogeneous system of linear equations has a nontrivial solution if the determinant of the corresponding system matrix is zero. It can be explicitly written as:

$$\Pi^T = T_{22} - T_{12}R_{dn} + T_{21}R_{up} - T_{11}R_{up}R_{dn} = 0. \tag{4}$$

A common practice is to search for the roots of the dispersion relation Π^T , Eq. (4), to obtain a set of eigen-frequencies. Assuming that a burner and its corresponding flame can be characterized separately, the definition of transfer matrix elements T_{ij} in Eq. (4) can be expressed as $\mathbf{T} = \mathbf{T^f T^B}$. Here, $\mathbf{T^f}$, $\mathbf{T^B}$ represent the transfer matrices of the flame and burner. It is shown [8] that for a wide range of so-called acoustic velocity sensitive flames there is direct relation between the entries of the $\mathbf{T^f}$ matrix and the flame heat release transfer function. In the limit of zero Mach number, this relation has the following form, $T^f_{11} = T^f_{22} = \frac{1}{2}\big(\epsilon + 1 + \theta\mathcal{F}\big)$ and $T^f_{12} = T^f_{21} = \frac{1}{2}\big(\epsilon - 1 - \theta\mathcal{F}\big)$. Here, $\theta = \frac{T_2}{T_1} - 1$ is the temperature jump, $\epsilon = \frac{\rho_{01}c_{01}}{\rho_{02}c_{02}}$ the specific impedance jump across the flame and $\mathcal{F}$ represents the flame transfer function. In the subsequent subsection, building upon the discussed low-order model of the generic combustion system thus far, we delve into the framework of burner-flame TM composition.

2.2 The framework of the burner-flame TM composition

In this subsection, the key procedures in the framework of the burner-flame TM composition are briefly explained separately. The entire framework can be done based on the tabulated library of characterized elemental burners.

2.2.1 Burner TM composition

According to Figure 2, for a generic two-partitioned composite burner conditions of acoustic pressure equilibrium and the principle of mass conservation at upstream and downstream side of the burner yield [9]:

$$p'_1 = p'^{(1)}_1 = p'^{(2)}_1, \qquad p'_2 = p'^{(1)}_2 = p'^{(2)}_2. \tag{5}$$

$$u'_1 = \alpha u'^{(1)}_1 + (1-\alpha)u'^{(2)}_1, \qquad u'_2 = \alpha u'^{(1)}_2 + (1-\alpha)u'^{(2)}_2, \tag{6}$$

here, $\alpha = A^c_1/A^c_B$ represents the partition area ratio, where A^c_B and A^c_1 denote the total area of the composite burner and the portion of the area occupied with the segment/partition identical to elemental burner 1, respectively. For instance, as illustrated in Figure 2(c), the upper half of the composite burner corresponds to elemental burner 1 (refer to Figure 2(a)). Thus, α can be calculated as 0.5. Assuming plane-wave propagation, the state variables upstream of the burner and the state variables downstream of the burner are related by:

$$\begin{bmatrix} p'^{(k)}_2 \\ u'^{(k)}_2 \end{bmatrix} = \overbrace{\begin{bmatrix} M^{(k)}_{11} & M^{(k)}_{12} \\ M^{(k)}_{21} & M^{(k)}_{22} \end{bmatrix}}^{[\mathbf{M}^{(k)}]} \begin{bmatrix} p'^{(k)}_1 \\ u'^{(k)}_1 \end{bmatrix}, \qquad k = 1, 2. \tag{7}$$

By considering Eqs. (5-7) the governing equations can be formulated. For the elemental burner 1,

$$p'_2 = M^{(1)}_{11}p'_1 + M^{(1)}_{12}u'^{(1)}_1, \qquad u'^{(1)}_2 = M^{(1)}_{21}p'_1 + M^{(1)}_{22}u'^{(1)}_1. \tag{8a}$$

For the elemental burner 2,

$$p'_2 = M^{(2)}_{11}p'_1 + M^{(2)}_{12}u'^{(2)}_1, \qquad u'^{(2)}_2 = M^{(2)}_{21}p'_1 + M^{(2)}_{22}u'^{(2)}_1 \tag{8b}$$

By Combining Eq. (6) and Eq. (8e), the total TM of the composite burner based on acoustic particle velocity and acoustic pressure can be summarized:

$$\begin{bmatrix} p'_2 \\ u'_2 \end{bmatrix} = \overbrace{\begin{bmatrix} M_{11} & M_{12} \\ M_{21} & M_{22} \end{bmatrix}}^{[\mathbf{M}]} \begin{bmatrix} p'_1 \\ u'_1 \end{bmatrix}, \tag{9}$$

where,

$$M_{11}^B = M_{11}^{(1)} + \frac{(1-\alpha)(M_{11}^{(2)} - M_{11}^{(1)})M_{12}^{(1)}}{(1-\alpha)M_{12}^{(1)} + \alpha M_{12}^{(2)}}, \qquad M_{12}^B = \frac{M_{12}^{(1)} M_{12}^{(2)}}{(1-\alpha)M_{12}^{(1)} + \alpha M_{12}^{(2)}}, \tag{10a}$$

$$M_{21}^B = \alpha M_{21}^{(1)} + (1-\alpha)M_{21}^{(2)} + \frac{(1-\alpha)\alpha(M_{22}^{(1)} - M_{22}^{(2)})(M_{11}^{(2)} - M_{11}^{(1)})}{(1-\alpha)M_{12}^{(1)} + \alpha M_{12}^{(2)}}, \qquad M_{22}^B = M_{22}^{(2)} + \frac{\alpha(M_{22}^{(1)} - M_{22}^{(2)})M_{12}^{(2)}}{(1-\alpha)M_{12}^{(1)} + \alpha M_{12}^{(2)}}. \tag{10b}$$

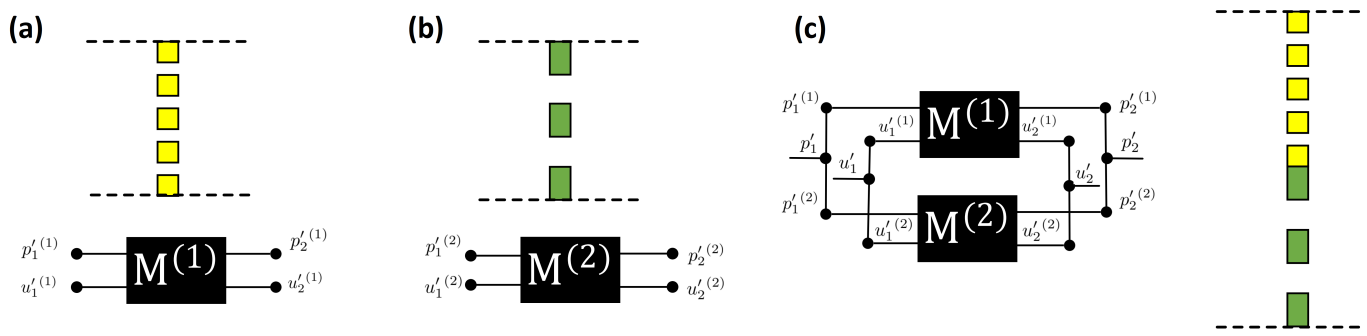

Figure 2: A sketch of (a), (b) two different generic uniform perforated burners and their corresponding two port representation; (c) a typical composite burner with two partitions identical with (a) and (b), along with the its corresponding two port representation.

To formulate of TM based on the Riemann invariants f_j and g_j as earlier defined, the following transformations are used:

$$T_{11}^B = \frac{1}{2}\Big(\frac{\rho_{01}c_{01}}{\rho_{02}c_{02}}M_{11}^B + \frac{M_{12}^B}{\rho_{02}c_{02}} + \rho_{01}c_{01}M_{21}^B + M_{22}^B\Big), \qquad T_{12}^B = \frac{1}{2}\Big(\frac{\rho_{01}c_{01}}{\rho_{02}c_{02}}M_{11}^B - \frac{M_{12}^B}{\rho_{02}c_{02}} + \rho_{01}c_{01}M_{21}^B - M_{22}^B\Big), \tag{11a}$$

$$T_{21}^B = \frac{1}{2}\Big(\frac{\rho_{01}c_{01}}{\rho_{02}c_{02}}M_{11}^B + \frac{M_{12}^B}{\rho_{02}c_{02}} - \rho_{01}c_{01}M_{21}^B - M_{22}^B\Big), \qquad T_{22}^B = \frac{1}{2}\Big(\frac{\rho_{01}c_{01}}{\rho_{02}c_{02}}M_{11}^B - \frac{M_{12}^B}{\rho_{02}c_{02}} - \rho_{01}c_{01}M_{21}^B + M_{22}^B\Big). \tag{11b}$$

2.2.2 The principle of flame TF composition

For the case of premixed, gaseous flames, the flame transfer function (TF) is defined as the ratio of the relative heat release rate perturbation ($\hat{Q}'/\bar{Q}$) and the relative flow perturbation ($\hat{u}'/\bar{u}$)

$$\mathcal{F}(\omega) = \frac{\hat{Q}'}{\hat{u}'}\frac{\bar{u}}{\bar{Q}}. \tag{12}$$

We first consider the general case of a composite burner deck, when the type of deck structure and flame pattern are not specified, to mathematically formulate the total flame/burner TF of a multi-flame burner from the superposition of the individual elemental patterns. By relating the local and global heat release rates of the TFs to the same upstream relative flow oscillation $\frac{u'}{\bar{u}}$. One can formulate the global/accumulative flame TF as follows [2, 6]:

$$\mathcal{F}_\Sigma(\omega) = \sum_{k=1}^{n_k} \mathcal{F}_k(\omega)\Omega_k. \tag{13}$$

where n_k is the number of grouped flames (usually equals to the number of partitions). The weight coefficients Ω_k of flame of group k indicate the distribution of thermal power among the partitions. The TF of the elemental flames $\mathcal{F}_k(\omega)$ need to be defines at the operating condition corresponding to the Ω_k and it is defined based on the concept of equal pressure drop that will be discussed in the next subsection.

2.2.3 A model for pressure drop (PD) composition

The pressure drop (PD) test vesus mass flow rate ($\dot{m}$) is essential for acquiring the necessary information for the TF composition. It essentially quantifies the flow passing through the various perforations across the burner deck. In this section, we discuss the model of PD composition, which enables the determination of the PD of composite burners based on the PD information of the elemental/basic burners constituting the composite burner. The pressure drop for elemental burners (Δp_k) and composite burners (Δp_c) can be expressed in the form of a quadratic polynomial, known as the Hazen-Dupuit-Darcy model or Forchheimer equation [10]:

$$\Delta p_c = c_{c1}\dot{m}_c + c_{c2}\dot{m}_c^2, \tag{14}$$

$$\Delta p_k = c_{k1}\dot{m}_k + c_{k2}\dot{m}_k^2, \qquad k = 1, 2, ..., n_k, \tag{15}$$

where k and n_k indicate an index for elemental burner and the number of elemental burners, respectively. Needless to say that the number of elemental burners is equal to the number of segments in the partitioned composite burner. The coefficients c_{k1} and c_{c1} are corresponding to the effect of viscous and inertial resistance factors for elemental and composite burners, respectively. Similarly, the coefficients c_{k2} and c_{c2} indicate the effect of inertial resistance factors for the elemental and composite burners. c_{k1} and c_{k2} are determined experimentally by fitting a curve to the measurements of pressure drop versus mass flow rate for the range of interest for mass flow rate. Using the conservation of mass law in the composite burner and using the concept iso-PD ($\Delta p_1 = \Delta p_2 = ... = \Delta p^{k-1} = \Delta p^k$), one can form $n_k - 1$ algebraic equations. For the sake of simplicity, we assume a composite burner with only two elemental partitions, and after solving these algebraic equations the mass flow rate through the different basic burners can be obtained as follows:

$$\dot{m}_1 = \frac{\dot{m}_c}{\alpha} + \frac{\beta_3 + (1-\alpha)\sqrt{\beta_1}}{\beta_2}, \tag{16a}$$

$$\dot{m}_2 = \dot{m}_c - \dot{m}_1. \tag{16b}$$

where

$$\beta_1 = \alpha^2 c_{11}^2 - 2\alpha^2 c_{11}c_{21} + \alpha^2 c_{21}^2 - 2\alpha c_{11}^2 + 2\alpha c_{11}c_{21} + 4\alpha c_{11}c_{22}\dot{m}_c - 4\alpha c_{12}c_{21}\dot{m}_c + c_{11}^2 + 4c_{12}c_{21}\dot{m}_c + 4c_{12}c_{22}\dot{m}_c^2, \tag{17a}$$

$$\beta_2 = 2(c_{12} - 2\alpha c_{12} + \alpha^2 c_{12} - \alpha^2 c_{22}), \tag{17b}$$

$$\beta_3 = -c_{11} + 2\alpha c_{11} - \alpha c_{21} + 4\dot{m}_c c_{12} - \alpha^2 c_{11} + \alpha^2 c_{21} - 2\alpha c_{12}\dot{m}_c - 2c_{12}\dot{m}_c/\alpha. \tag{17c}$$

3. Numerical example

The concept of flame TF composition and the model for PD composition have already been experimentally validated [6]. Here, we initially demonstrate the validation of the formulation concerning the concept of the burner TM composition. Subsequently, we showcase the framework of the burner-flame TM composition in flame stabilization, utilizing a classical duct-flame-duct benchmark test case.

Burner TM composition

To demonstrate the validity of the formulation and assumptions presented in the previous section regarding the development of the burner TM composition, we consider two elemental burners with slits of different widths and acoustic absorbing characteristics, as illustrated in Figure 3. For simplicity, we assume that the effect of mean flow on the TM of burners in the vicinity of zero Mach number is negligible. Utilizing the Helmholtz equation solver in COMSOL, specifically the module of *pressure acoustics*, we compute the TM of different burners separately, taking into account thermoviscous effects in a very narrow region along the perforation. Subsequently, we employ the concept of burner TM composition, as outlined in Eqs. (9)-(10), to obtain the TM of two composite burners with $\alpha = 0.5$ and $\alpha = 2/3$. To assess the accuracy of the model, we conducted a direct evaluation of the TM of composite burners. The results, presented in Figure 4, demonstrate an excellent agreement across the entire frequency range of interest.

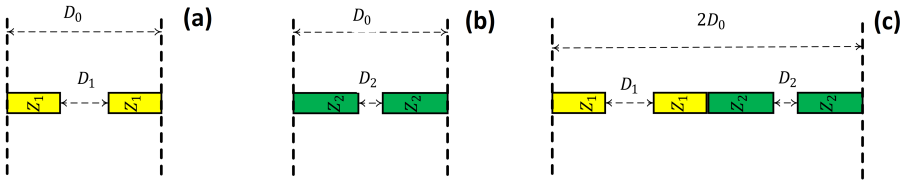

Figure 3: Sketch of two elemental burners (B1 and B2) with slits of different widths and one partitioned composite burners with $\alpha = 0.5$. (a) $z_1 = \rho_{01}c_{01}$ Pa $\cdot$ s/m , $D_1 = 0.5$ mm and $D_0 = 4$ mm; (b) $z_2 = 0.5\rho_{01}c_{01}$ Pa $\cdot$ s/m , $D_2 = 0.25$ mm and $D_0 = 4$ mm.

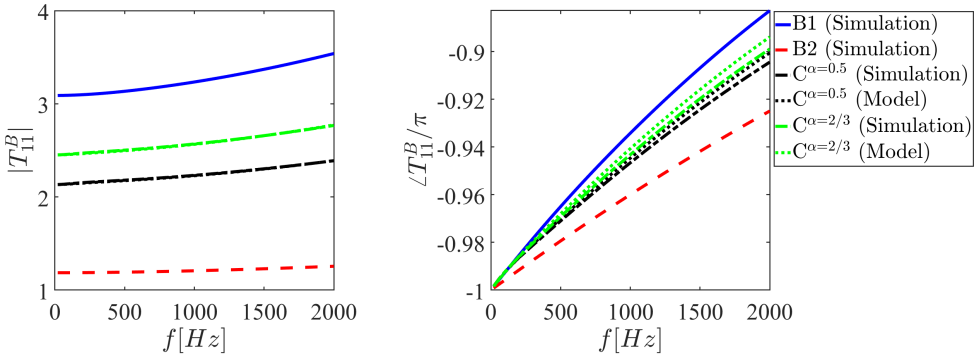

Figure 4: The first entries of the burners' TM T_{11}^B for elemental burners and the partitioned composite burners.

Application of the burner-flame TM composition in stabilization of thermo-acoustic system

To apply the framework of burner-flame TM composition in the context of thermoacoustic instability, it is instructive to consider a generic thermoacoustic system that mimics the model shown in Fig. 1. As a benchmark-like example, we consider the test case shown in Fig. 5 with an upstream and downstream lengths $L_1 = 0.1$ m and $L_2 = 0.1$ m, respectively. The end terminations of upstream and downstream are considered as frequency-independent and purely real end reflections $R_1^e = -0.3$ and $R_2^e = -0.5$, respectively. The total acoustic reflection up- and downstream of the flame can be lumped:

$$R_{up} = R_1^e e^{-2i\omega L_1/c_{01}}, \qquad R_{dn} = R_2^e e^{-2i\omega L_2/c_{02}}. \tag{18}$$

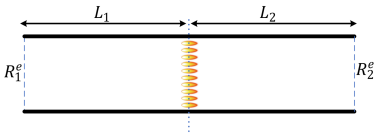

Figure 5: Sketch of a uniform duct-flame-duct geometry.

In the current study for the sake of simplicity, a theoretical PD model has been used [11] to estimate the PD of the elemental burners:

$$\Delta P = \frac{1}{2} c_2' \rho u^2, \qquad c_2' = (0.707(1-\eta)^{0.375} + 1 - \eta)^2/\eta^2, \tag{19}$$

where, η indicates the porosity of the elemental burners and can be calculated as the ratio of open area to the total area of the burner. Using PD data, as shown in the Figure 6, one determines the distribution of thermal power.
It is known that the thermoacoustic behavior of many practical flames can be described by the transfer function simplified based on the hybrid empirical-theoretical model as follows [12]:

$$\mathcal{F} = e^{-i\omega\tau} e^{0.5(-i\omega)^2\sigma^2}, \qquad \sigma = 0.35\tau. \tag{20}$$

where, $\tau = KH$ indicates the time delay, and we assumed it has a linear correspondence to the height of the flame ($K = 0.5\mathrm{s/m}$), and the height of flame can be simplified as follows [8]:

$$H = \frac{D_p}{2}\left(\left(\frac{u_p}{S_L}\right)^2 - 1\right)^{0.5}, \tag{21}$$

where, D_p, u_p and $S_L = 0.37$ m/s represent the width of slit in the burner, the velocity of fresh mixture in the slit and laminar flame speed, respectively. In the present work, D_p is known from the characteristics of elemental burners, as discussed in the previous subsection. The velocity u_p is calculated using the concept of iso pressure drop, and it heavily depends on the characteristics of the partitioned (integrated) composite burners α. To form the transfer matrix, knowledge of upstream and downstream temperature are required. Therefore, a fixed value of $T_1 = 300$ K is assumed, and a uniform temperature of $T_2 = 1900$ K representative of a realistic temperature for the downstream part of the duct.
Figure 6 illustrates the pressure drops of two elemental burners and one obtained from the PD model for the partitioned composite burner. This graph enables one to determine, at different inflow velocities, how much flow is directed to the various segments/partitions, thereby providing the necessary entries for the flame TF. Figure 7 compares the flame TFs of different composite burners (C$^{\alpha=0.4}$, C$^{\alpha=0.5}$, and C$^{\alpha=0.7}$) with elemental burners (constructed from burner 1, C$^{\alpha=1}$, and from burner 2, C$^{\alpha=0}$) at the same inflow velocity. It is evident that the global acoustic response of the flame, accumulated from different distributions of flames, can vary significantly in both gain and phase. This observation underscores the potential for flame stabilization through a systematic

approach based on a tabulated library of pressure drop, flame TF and TM of elemental burners. To further elucidate this opportunity, we conduct a stability analysis of the duct-flame-duct system equipped with various synthesized burners, as depicted in Figure 8. By solving the dispersion relation, Eq. (4), one can obtain the complex eigenfrequencies of the system. The imaginary part of the complex frequencies indicate the frequency of the thermoacoustic mode, while the real part indicate the growth rate, serving as an indicator of system stability. A positive value of σ indicates that oscillations in the system are growing exponentially, potentially leading to a limited cycle. Practically speaking, through passive control of thermoacoustics, we aim to eliminate this instability by modifying the flame properties. The graph illustrates that, under the considered operating conditions, elemental burners made from the burner 1 ($\alpha = 1$) and from the burner 2 ($\alpha = 0$) operate thermoacoustically unstable, indicated by the label U in the legend of Figure 8. Additionally, there exists a safe/stable combinations of burner 1 and burner 2 to integrate partitioned composite burners, which provide thermoacoustic stability. Specifically, composite burners with between 20% and 60% of the total area occupied with the burner 1 type partition and the rest occupied with burner 2 type partition are predicted to perform stable, denoted by the label S in the legend of Figure 8. On the contrary, composite burners with $\alpha = 0.7$, 0.8, and 0.9 are predicted to lead the system to instability.

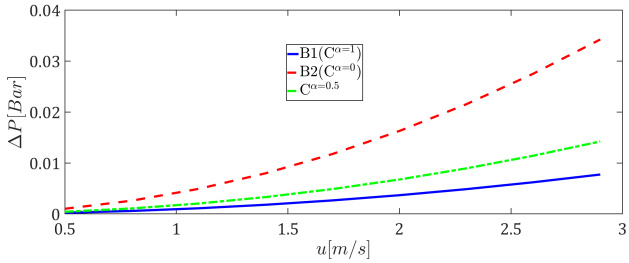

Figure 6: The pressure drop versus inflow velocity of elemental burners and a composite burner with $\alpha = 0.5$.

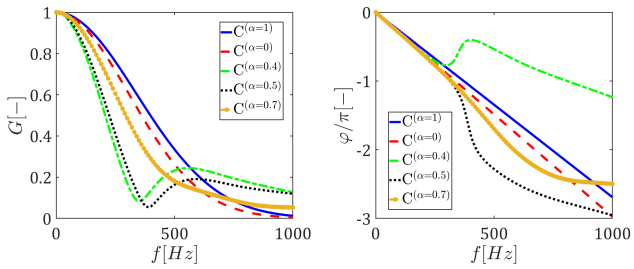

Figure 7: A view of the flame transfer functions of elemental burners and the composite burners at $u_{in} = 0.5$ m/s .

Most of combustion systems should be designed to operate over a wide range of thermal power. Therefore, a stability chart, as shown in Figure 9, is valuable. This chart clearly indicates stable choices marked with circles in blue and unstable choices shown with crosses in red, providing a comprehensive overview of combination choices to serve as a guideline. Such a tool is highly useful in the practical R&D process of burner development, especially considering the numerous requirements for modulation range, pressure drop restrictions, emissions, and stable combustion dynamics. Designers can weigh these requirements and make informed decisions to achieve the most optimized design.

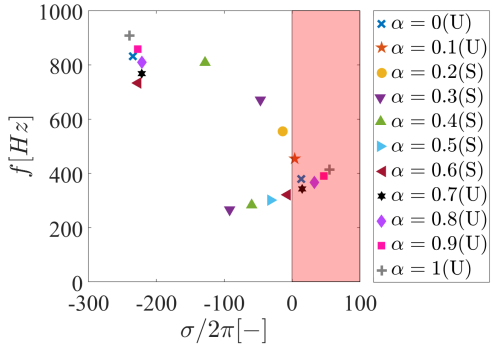

Figure 8: Eigen-modes of the duct-flame-duct system with the characteristics of $l_1 = 0.1$ m, $R_1^e = 0.3$, $l_2 = 0.1$ m and $R_2^e = -0.5$ when equipped with the various composite burners with their corresponding flame at inflow mixture velocity $u_{in} = 0.5$ m/s. Positive growth rate (σ) indicates an unstable mode. The labels U and S in the legens refer to unstable and stable configurations, respectively.

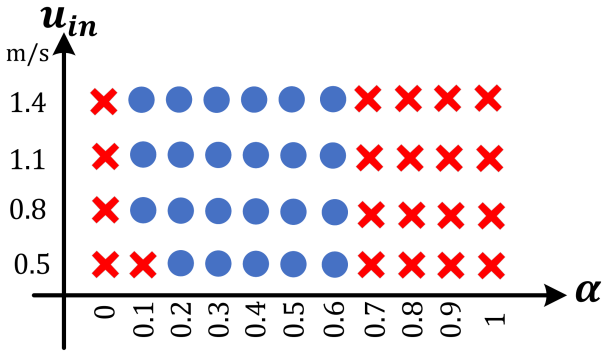

Figure 9: The stability chart for the duct-flame-duct system shown with the characteristics of $l_1 = 0.1$ m, $R_1^e = 0.3$, $l_2 = 0.1$ m and $R_2^e = -0.5$ when equipped with the various composite burners with their corresponding flame in different inflow mixture velocities.

4. Conclusions

Our study highlights the intricate relationship between burner design, flame characteristics, and thermoacoustic stability within combustion systems. We have introduced a novel approach aimed at addressing thermoacoustic instabilities by targeting the thermoacoustic properties of the burner and its corresponding flame. Through the concept of burner-flame transfer matrix composition, we have presented a systematic framework for designing optimized burners that operate thermo-acoustically stable while meeting various operational requirements. The analysis of a duct-flame-duct case study exemplifies the effectiveness of our approach. Additionally, the development of a stability chart provides valuable guidance for burner development, delineating safe and unsafe combinations of partitions. Overall, our research contributes to advancing the understanding and practical application of passive control strategies for thermoacoustic stability in combustion systems.

REFERENCES

1. Kelsall, G. and Troger, C. Prediction and control of combustion instabilities in industrial gas turbines, *Applied Thermal Engineering*, **24** (11-12), 1571–1582, (2004).

2. Kornilov, V., Manohar, M. and de Goey, L. Thermo-acoustic behaviour of multiple flame burner decks: Transfer function (de) composition, *Proceedings of the Combustion Institute*, **32** (1), 1383–1390, (2009).

3. von Saldern, J. G., Reumschüssel, J. M., Beuth, J. P., Paschereit, C. O. and Oberleithner, K. Robust combustor design based on flame transfer function modification, *International Journal of Spray and Combustion Dynamics*, **14** (1-2), 186–196, (2022).

4. Schuller, T., Durox, D. and Candel, S. A unified model for the prediction of laminar flame transfer functions: comparisons between conical and v-flame dynamics, *Combustion and flame*, **134** (1-2), 21–34, (2003).

5. Kagiya, S. New burner design technique for suppression of combustion oscillations, tokyo-gas co., *Energy and Environmental Technology Laborator*, (2000).

6. Ganji, H., Kornilov, V., van Oijen, J. and Arteaga, I. Characterization and identification of thermoacoustic behavior of flames anchored on burner decks with multiple perforations; transfer function (de)composition approach, Internoise 2022 - 51st International Congress and Exposition on Noise Control Engineering, (2022).

7. Munjal, M. L., *Acoustics of ducts and mufflers with application to exhaust and ventilation system design*, John Wiley & Sons (1987).

8. Hoeijmakers, P., *Flame-acoustic coupling in combustion instabilities*, Ph.D. thesis, Mechanical Engineering, proefschrift, (2014).

9. Selamet, A. and Easwaran, V. Modified herschel–quincke tube: Attenuation and resonance for n-duct configuration, *The Journal of the Acoustical Society of America*, **102** (1), 164–169, (1997).

10. Dukhan, N., *Metal foams: fundamentals and applications*, DEStech Publications, Inc (2013).

11. Idelchik, I. Handbook of hydraulic resistance, *Journal of Pressure Vessel Technology*, **109** (2), 260–261, (1987).

12. Schuermans, B. EPFL, Modeling and control of thermoacoustic instabilities, (2003).